Ref.TH.1932-CERN

FINAL STATE ABSORPTION IN MULTIPERIPHERAL MODELS

M. Ciafaloni*) and G. Marchesini

CERN - Geneva

ABSTRACT

We study s-channel unitarity effects in multiperipheral production amplitudes due to final state particle rescattering. For non-diffractive events we show that - if the Pomeron is required to have $\alpha(0) = 1$ - the absorbed overlap function leads to $\sigma_{in} \sim (\ell n\ s)^{\eta}$ and forward peak shrinking as $(\ell n\ s)^{\nu}$ similarly to Reggeon field theories. Inclusive many-particle distributions and production cross-sections are calculated, and found to have logarithmic multiplicity and integrable, i.e., not very long-range, correlations in the inelastic component. The t-distribution for diffractive production of large masses is found to have no turnover at small t in the model, but the probability of large-gap events is damped by absorption, so that consistency with unitarity is achieved. By the same token the Finkelstein - Kajantie paradox is avoided and multiple diffractive events give at most a small intercept renormalization. A comparison of this s-channel point of view with Reggeon field theory is also given.

*) Present address: Scuola Normale Superiore, Pisa, Italy.

Ref.TH.1932-CERN
25 September 1974

1. INTRODUCTION

Diffraction scattering in the NAL-ISR energy range is roughly characterized by the trend of all total cross-sections to increase (the more exotic, the first) and by the existence in inclusive distributions of sizeable correlations of short- and long-range type [1]. Two- and many-component models have been constructed [2] which connect these features to the existence of diffractive excitation of resonances and large masses.

The common idea behind these models is that there is a basic short-range order component (bare Pomeron) which, in a multiperipheral model, is a Regge pole coming from the iteration of low-energy interactions (Fig. 1), and giving a roughly constant cross-section. To this one has to add various diffractive and absorptive effects (Fig. 2) characterized by small parameters, like $\sigma_{diff}/\sigma_{tot} \simeq \sigma_{el}/\sigma_{tot} \simeq 1/5$. A perturbative treatment of these effects can give rise at the same time to both the increase in the total cross-sections and to the long-range correlations in production amplitudes.

The simple idea is made complicated by the requirement of s- and t-channel unitarity. We mention two points in this respect.

a) The simplest multiperipheral models (no absorptive effects at all) are consistent with the Froissart bound for the observed rise of the Pomeron interaction vertex $g_p(0,0,0)$ (Fig. 3) only for asymptotically decreasing σ_{tot} [3]. (The observed increase is attributed to a huge threshold effect.) Moreover, these models predict a positive Pomeron cut sign, contrary to t-channel [4] and s-channel arguments [5].

b) Models which include absorptive corrections and give negative cut sign are ambiguous. One of these ambiguities is the relative importance of s-channel versus t-channel iterations. Given the fact that σ_{tot} is increasing, these models assume at some stage a (bare) Pomeron intercept $\alpha_o > 1$. The problem then arises of whether it is the s-channel iteration [6] or the t-channel renormalization [7] which prevents violation of the Froissart bound. The physical predictions are different in the two cases, and a variety of models have been constructed giving various admixtures of these points of view [8].

This paper is a study of a particular s-channel unitarity effect, i.e., the absorption coming from elastic rescattering of pairs of produced particles. We shall argue that this gives rise to a negative intercept renormalization and, provided α_o and g_p are properly related, an absorbed scattering amplitude comes out which is basically similar to a Regge pole. It has factorized cross-sections increasing like $(\ell n\ s)^n$, logarithmically

increasing multiplicity, and single components of basically short-range order. These features are in agreement with t-channel approaches like the Reggeon field theories [7] where the logarithmic deviations from a pure pole behaviour have first been found [9),10)].

The occurrence of the previous results in an absorptive model comes at first sight as a surprise because prototype calculations [6),11)] are known to give rise to an asymptotic black disk and strongly modify both factorization properties and multiplicity distributions.

Let us recall the argument in the example of the Finkelstein-Zachariasen model [6)]. The overlap function $A(\underline{B},Y)$ in impact parameter, rapidity representation is written as

$$A = \frac{1}{2} A^2 + A^{(0)}(\underline{B},Y)\, R \quad , \tag{1.1}$$

where $A^{(0)}$ is given via unitarity by a $2 \to N$ transition amplitude (e.g., multiperipheral) and

$$R = S(\underline{B},Y) = 1 - A(\underline{B},Y) \, . \tag{1.2}$$

If one assumes that the bare Pomeron $A^{(0)}$ (a complex potential in the game) is a Regge pole with intercept higher than 1, i.e.,

$$A^{(0)} = \beta_A \beta_B \, e^{\delta Y} \, \frac{e^{-\underline{B}^2/4\alpha' Y}}{4\alpha' Y} \quad , \quad \delta = \alpha_0 - 1 > 0 , \tag{1.3}$$

the unitarity bound is asymptotically violated for

$$\underline{B}^2 \lesssim 4\alpha' \delta \, Y^2 \, . \tag{1.4}$$

This forces the rescattering factor $R = S$ to vanish in that range, giving rise to the (expanding) black disk picture, and to saturation of the Froissart bound.

The model we are going to discuss is, on the other hand, defined [12)-14)] in terms of the $2 \to N+2$ production amplitudes in the impact parameter representation *) (Fig. 4)

---

*) There is a controversy on whether Eq. (1.5) should be written with factors of S or $S^{\frac{1}{2}}$. The choice of S is supposed to be proper for non-planar graphs, but is also not free of criticism in that case (T. Degrand, MIT preprint). We therefore choose $S^{\frac{1}{2}}$ as in the naive absorption model, in order to reproduce the counting 1: -2 of diffractive versus absorptive discontinuities of that model. This differs from previous papers [Refs. 12, 13)], where however the normalization was unimportant because only one kind of events (absorptive or diffractive) was considered.

$$A_N(\underline{b}_1, y_1; \ldots; \underline{b}_N, y_N; \underline{B}, Y) = A_N^0 \prod_{i>j}^{N} S^{1/2}(\underline{b}_i - \underline{b}_j, y_i - y_j), \quad (1.5)$$

where A_N^0 is assumed to be a multiperipheral matrix element. The partial wave unitarity equation for this model is much more complicated than (1.1), and its detailed analysis is the main purpose of this paper. A rough comparison with (1.1) can be obtained by the replacement

$$R \to \langle R \rangle = \Big\langle \prod_{i>j} |S_{ij}| \Big\rangle \simeq \Big\langle e^{-\sum_{i>j} A_{ij}} \Big\rangle , \quad (1.6)$$

where the average is defined over the weight $|A_N^0|^2/A^0$.

It is clear that in (1.6) the absorption is enhanced by a multiplicity effect. Since there are $\sim \frac{1}{2}N^2$ terms in the sum, and each term is of order $1/Y$ for a pure Regge pole, it follows that (1.6) is roughly of order

$$\langle R \rangle \simeq \exp\left(-\text{const}\, N^2/Y\right) , \quad (1.7)$$

which for $\langle N \rangle \sim GY$ can be arranged to cancel the $e^{\delta Y}$ factor in $A^{(o)}$ by a proper choice of the couplings. In other words, one can arrange $\Pi_{i>j}|S_{ij}|$ to vanish as $Y \to \infty$ at the desired rate, even if $S_{ij} = 1 + O(1/Y)$ as it happens for a Regge-like amplitude.

It turns out that the argument given before is only roughly correct, due to the long-range nature of the Pomeron exchange ($\sim 1/Y$), and that $Y^h(\ell n\, Y)^k$ terms actually arise in the exponent of (1.6) (subsection 2.2). This singular behaviour means that a pure Pomeron pole is not self-consistent if -- as it happens for a pure multiperipheral model of the bare pole -- the coupling $g_p(0,0,0) \neq 0$. We are therefore faced with the non-perturbative problem of summing the $Y^h(\ell n\, Y)^k$ terms and finding out the actual self-consistent $A(\underline{B}, Y)$.

This problem is approximately solved in the paper (subsection 2.3) by using $\underline{b}$, Y variables and s-channel concepts. It admits a parallel treatment in the t-channel, in a form similar to, but not identical with Reggeon field theories [9),10)] (RFT). We defer to the conclusion a thorough discussion of the two approaches, but we note the encouraging fact that both s- and t-channel treatments give rise to qualitatively similar results.

The starting point for solving the unitarity equation related to (1.5) is the functional identity

$$\exp\left\{\int dv_1\, dv_2\, \ln|S(v_2-v_1)|\,\frac{\delta^2}{\delta\varphi(v_1)\delta\varphi(v_2)}\right\}\prod_{i=1}^{N} e^{\varphi(v_i)} = \prod_{i>j}|S_{ij}|\prod_{i=1}^{N} e^{\varphi(v_i)}, \tag{1.8}$$

where $v_i \equiv (\underline{b}_i, y_i)$ and $dv = 2d\underline{b}\,dy$. By defining the generating functional of v-distributions $[V \equiv (\underline{B}, Y);\ v_0 \equiv (\underline{0}, 0)]$

$$G_{v_0 V}(\psi) \equiv \sum_N \int dv_1 \cdots dv_N \left| A_N(v_0, v_1, \ldots, v_N, V)\right|^2 \prod_{i=1}^{N}(1+\psi(v_i)), \tag{1.9}$$

and analogously for A_N^0, G^0, we get

$$G_{v_0 V}(e^{\varphi}-1) = \exp\left\{\int dv_1\, dv_2\, \ln|S_{12}|\,\frac{\delta^2}{\delta\varphi_1\delta\varphi_2}\right\} G^0_{v_0 V}(e^{\varphi}-1), \tag{1.10}$$

$$G_{v_0 V}(\psi=0) = A_{in}(V-v_0) = A(V-v_0) - \tfrac{1}{2}A^2(V-v_0),$$

where

$$\ln|S(v)| = -A(v) + O(A^2). \tag{1.11}$$

Equations (1.10) and (1.11) are non-linear integral equations for $A(v)$ and a knowledge of the multiperipheral generating functional G^0 allows, in principle, to write them explicity. Note that for the asymptotic calculations we perform here $A(v) \ll 1$, so that further terms A^n occurring in (1.11) (for $S = 1 - A$) do not really matter. The precise expression for S is, however, crucial if we look for solutions for which $A \simeq 1$ asymptotically.

Since Eq. (1.10) gives the physical generating functional for the absorbed amplitude, one can obtain (once A_{in} is calculated) all particle inclusive distributions at no extra cost.

The plan of the paper follows logically the gap expansion [15]. We first assume that A_N^0 contains only short-range interactions (no large-gap events). We discuss how to obtain an approximate asymptotic $A_{in}(V)$ in Section 2. In particular, we discuss how the non-linear equations of our model can be solved in the ϵ-expansion [16]. In Section 3 we calculate vertex corrections and physical inclusive distributions in the plateau region. We also give a simple treatment of rescattering for fixed numbers of produced particles. In Section 4 we introduce diffractive excitation in A_N^0 and discuss absorptive corrections for the triple-Pomeron formula. We also comment on the

resulting modifications of the fireball expansion. In the conclusive Section 5 we give a summary of the results and a comparison with other approaches.

2. OVERLAP FUNCTION FOR NON-DIFFRACTIVE EVENTS

2.1 Description of the model

In order to obtain the functional $G(\psi)$ from Eq. (1.10), a specific form for the bare functional $G^{(o)}(\psi)$ has to be assumed. In this section we concentrate on describing the model for non-diffractive events, i.e., events in which particles are produced without large rapidity gaps (single fireball).

For the bare production amplitude $A_N^{(o)}$ we assume a short-range model, like a multiperipheral model without Pomeron exchanges (Fig. 1), which gives rise to a bare overlap function $A^{(o)}(V - v_o)$ given, for large rapidity, by a Pomeron pole with intercept $\alpha_o > 1$:

$$A^{(o)}(V-v_o) \equiv \beta^2 e^{\delta Y} \frac{e^{-\underline{B}^2/Y}}{2\pi Y} \equiv \beta^2 e^{\delta Y} F(V-v_o) \,, \qquad (2.1)$$

where $\delta = \alpha_o - 1$, $4\alpha' = 1$, and $V \equiv (Y, \underline{B})$, $v_o \equiv (0, \underline{0})$. The bare functional $G^o_{v_o V}(\psi)$, defined in Eq. (1.9) with bare multiperipheral amplitudes A^o_n, due to the general factorization properties of A^o_n can be expressed as

$$G^{(0)}_{v_0 V}(\psi) = \sum_n \int dv_1 \cdots dv_n \; \psi(v_1) \cdots \psi(v_n) \prod_{i=1}^{n+1} A^{(o)}(v_i - v_{i-1}) \,, \qquad (2.2)$$

with $v_{n+1} = V$. From this form of $G^o(\psi)$ we can define the inclusive distributions in the v-space, for large rapidity differences:

$$\rho^{o\,(1)}_{v_0 V}(v) = \frac{A^{(o)}(v-v_o)\, A^{(o)}(V-v)}{A^{(o)}(V-v_o)} = G \frac{F(v-v_o)\, F(V-v)}{F(V-v_o)} \,, \qquad (2.3)$$

$$\rho^{o\,(2)}_{v_0 V}(v_1 v_2) = G^2 \frac{F(v_1-v_o)\, F(v_2-v_1)\, F(V-v_2)}{F(V-v_o)} + (v_1 \rightleftarrows v_2) \,,$$

etc., where for simplicity we have set $G = \beta^2$. The inclusive y-distributions $\rho^{o(n)}_Y(y_1 \cdots y_n)$ in the plateau region are related to $\rho^{o(n)}_{v_o V}$ by

$$\rho_Y^{o(n)}(y_1 \cdots y_n) = \frac{1}{\sigma_{in}(Y)} \int 2d\underline{B}\, 2d\underline{b}_1 \cdots 2d\underline{b}_n\, \rho_{v_o V}^{o(n)}(v_1 \cdots v_n)\, A^{(o)}(V - v_o) \qquad (2.4)$$

$$\simeq G^n \quad , \quad \text{for} \quad |y_i - y_j| \gg 1 \quad ,$$

consistently with our short-range order ansatz.

From Eq. (2.2) we have the interpretation of $G^o(\psi)$ as a propagator in the v-space of a non-relativistic field with an energy momentum gap δ [bare Pomeron $A^{(o)}$] in presence of an external source $\psi(v)$ (cf. Fig. 5). From Fig. 5 it is easy to obtain a graphical representation of the functional $G(\psi)$. From Eq. (1.10), by replacing $\phi(v)$ with $\psi(v) \equiv e^{\phi(v)} - 1$, we get in fact

$$G(\psi) = \exp\left\{ \int (1+\psi_1) \frac{\delta}{\delta \psi_1} (1+\psi_2) \frac{\delta}{\delta \psi_2} \ln |S_{12}| \right\} G^{(o)}(\psi) \,, \qquad (2.5)$$

$$= K\, G^{(o)}(\psi) \quad ,$$

with $G_{v_o V}(0) = A_{in}(V - v_o) \simeq A(V - v_o)$, and $S(v) = 1 - A(v)$. The action of the functional differential operator K is to connect any pair of points v_i, v_j in Fig. 5 with the rescattering function $\ln|S(v_i - v_j)$ and to replace $\psi(v)$ with $1 + \psi(v)$. Any point v can then be differentiated and connected with other points an infinite number of times. The overlap function $A(V - v_o)$ is then given by a sum of graphs of type in Fig. 6.

The non-linear aspect of this rescattering model is evident in Fig. 6: the solution $A(V - v_o)$ (output Pomeron) is also entering in the rescattering function $\ln|S(v_i - v_j)| \simeq -A(v_i - v_j)$. This non-linear problem can be approached in an iterative scheme by assuming a specific form for the rescattering function $\ln|S|$. From the discussion in the Introduction, we expect that (except for an intercept renormalization) the solution $A(v)$ does not differ greatly from the bare Pomeron $A^{(o)}(v)$ in Eq. (2.1). We assume then, for the rescattering function, the asymptotic form of a bare Pomeron with $\alpha(0) = 1$ and a slope $\beta' = r\alpha'$

$$\ln|S(v)| \simeq -A(v) \simeq -g^2 F_r(v) \quad , \quad (y > \Delta) \,, \qquad (2.6)$$

$$F_r(v) \equiv F(\underline{b}, ry) \,.$$

In this first iteration the output Pomeron $A(v)$ is then given by a sum of renormalization graphs of the type in Fig. 7, in which the Pomerons in the right-hand side are all bare. Since a particle in the intermediate state of a cut bare Pomeron can rescatter several times with other produced

particles, in the graphs of Fig. 7 there are, in general, many Pomeron vertices; a vertex with n rescattering Pomerons is associated with a coupling proportional to g^n. However, to a given order of g, the graphs with only three Pomeron vertices are asymptotically dominating. Graphs of Fig. 7 with only these vertices are a part of the full set of renormalization graphs of a three-Pomeron interaction RFT [9),10)]. The essential difference is that the rescattering bare Pomeron is not renormalized [except for being $\alpha(0) = 1$].

2.2 Generating functional and overlap function to order g^2

The functional $G(\psi)$ to order g^2 can be easily obtained from Eqs. (2.5), and is simply given by

$$G(\psi) = G^{(0)}(\psi) - g^2 \int dv' dv'' \, F_r(v'-v'') \, (1+\psi(v'))(1+\psi(v'')) \times \frac{\delta^2}{\delta\psi(v')\delta\psi(v'')} \, G^{(0)}(\psi) + O(g^4) \,, \tag{2.7}$$

which gives for the output Pomeron

$$A(V-v_0) = A^{(0)}(V-v_0) \left(1 - g^2 \int dv' dv'' \, F_r(v'-v'') \, \rho^{o(2)}_{v_0 V}(v'v'') + O(g^4) \right) = A^{(0)}(V-v_0) \, R_{v_0 V} \,. \tag{2.8}$$

Similarly we can compute the output v-distributions defined by

$$A(V-v_0) \, \rho^{(n)}_{v_0 V}(v_1 \dots v_n) \equiv \frac{\delta^n}{\delta\psi(v_1) \dots \delta\psi(v_n)} \, G_{r\, v_0 V}(\psi) \Big|_{\psi=0} \,, \tag{2.9}$$

and we obtain

$$A(V-v_0) \, \rho^{(n)}_{v_0 V}(v_1 \dots v_n) = A^{(0)}(V-v_0) \Big\{ \rho^{o(n)}_{v_0 V}(v_1 \dots v_n) - g^2 \Big[\int dv' dv'' \, F_r(v'-v'') \, \rho^{o(n+2)}_{v_0 V}(v_1 \dots v_n \, v' v'') + \sum_i \int dv' \, F_r(v'-v_i) \, \rho^{o(n+1)}_{v_0 V}(v_1 \dots v_n \, v') + \sum_{i,j} F_r(v_i - v_j) \, \rho^{o(n)}_{v_0 V}(v_1 \dots v_n) \Big] + O(g^4) \Big\} \,. \tag{2.10}$$

The interpretation of the various terms of the corrections to $\rho^{(n)}$ is given in Fig. 8 for the two-particle distribution. Only the contribution of graphs a and b corresponds to enhanced cuts in the Gribov language.

From Eq. (2.8) we can compute the absorbed cross-section $\sigma_{in}(Y)$ to order g^2 and we get

$$\sigma_{in}^{AB}(Y) = \beta_A \beta_B e^{\delta Y} \left(1 - \frac{g^2 G^2}{2\pi} \frac{r}{1+r} Y \ln Y + O(g^4) \right) . \qquad (2.11)$$

This contribution (Fig. 9a), for $\delta = 0$ and $r = 1$, reproduces the second-order Gribov graph of Fig. 9b provided that the three-Pomeron coupling $g_P^{(0)}$ (bare coupling) is related to g by

$$g_I^{(0)} = g G \ . \qquad (2.12)$$

As in the Gribov calculus we have then that the g^2 term in $A(V)$ gives a singular contribution to renormalization. This fact shows that higher g^2 terms are important in Eqs. (2.7), (2.8) and (2.10), and a non-perturbative calculation is needed.

2.3 Non-perturbative approach and ε-expansion

Possible non-perturbative treatments of Eq. (2.5) are centred around two ideas.

i) There exist solutions which admit scaling properties in $\underline{B}, Y$ variables, i.e., of the form

$$A(\underline{B}, Y) = Y^{\eta - \frac{d}{2}\nu} f\left(\underline{B}^2 / Y^{\nu} \right) , \qquad (2.13)$$

where d is the number of transverse dimensions ($\underline{B}$ space), as proposed by Gribov and Migdal [7] in the RFT.

ii) The "critical exponents" η and ν can be expanded in the parameter $\varepsilon = 4 - d$ starting from the values $\eta = 0$, $\nu = 1$ (pure Regge pole) for $d = 4$ [ε-expansion [16]].

We have already mentioned that the first approximation of Fig. 7, in the iterative approach, is equivalent to a RFT in two transverse dimensions, where the unrenormalized rescattering Pomeron field ψ_o (input Regge pole) is in interaction with the first-order output field ψ_1 with $i g_P^o \psi_1^+ \psi_1 \psi_o$ interaction. This problem, treated by renormalization group methods in the literature [17], admits a solution of form (2.13) with

$$\eta \simeq \gamma - 1 \simeq \varepsilon/4 \quad . \tag{2.14}$$

A different approach [18], leading to the same result, is to start from the equation

$$\frac{d}{dg^2} A(V-v_0;g^2) = -A(V-v_0;g^2) \int dv_1\, dv_2\, F_r(v_2-v_1)\, \rho^{(2)}_{v_0V}(v_1 v_2;g^2) , \tag{2.15}$$

which is easily derived from Eq. (2.5) within the iterative approximation (2.6) and with the definition

$$\rho^{(2)}_{v_0V}(v_1 v_2) = \frac{1}{A(V-v_0;g^2)} \left. \frac{\delta^2 G_{v_0V}(\psi)}{\delta\psi(v_1)\,\delta\psi(v_2)} \right|_{\psi=0} , \tag{2.16}$$

which gives the renormalized pair density in $\underline{b},y$ space [cf. Eq. (2.9)].

Equation (2.15) has the formal solution

$$A(V-v_0;g^2) = A^{(0)}(V-v_0)\, R_{v_0V} , \tag{2.17}$$

where the rescattering factor R_{v_0V}, which takes into account all absorptive effects, is defined by

$$R_{v_0V} = \exp\left\{ - \int dv_1\, dv_2\, F_r(v_2-v_1) \int_0^{g^2} dg'^2\, \rho^{(2)}_{v_0V}(v_1 v_2;g'^2) \right\} , \tag{2.18}$$

and is a generalization of the second-order result of Eq. (2.8). Similar generalization of Eq. (2.18) for $\rho^{(n)}$ distributions can be obtained and are discussed in the next section.

The effect of absorptive corrections in $\rho^{(2)}$ is that of softening, at large rapidity difference, the rescattering function $F_r(v_2 - v_1)$ and damping its slow decrease ($F_r(v) \sim 1/y$), which was the cause of the $Y\ \ell n\ Y$ divergence found in the second-order calculation in Eq. (2.11). It has been shown in Ref. 18) that the screening at large rapidity due to $\rho^{(2)}$ in Eq. (2.18) is consistent with the screening of vertices in $\rho^{(2)}$ if the rescattering factor R_{v_0V} is asymptotically scale invariant in rapidity *),

*) The dependence on the rapidity difference $y_2 - y_1$ only is true to leading order in the ϵ-expansion (cf. M. Ciafaloni and S. Ferrara, in preparation, for a direct justification on the relativistic Dyson equation).

i.e.,

$$\int d\underline{b}_1\, d\underline{b}_2\, F_r(v_2-v_1)\int_0^{g^2} dg'^2\, \rho^{(2)}_{v_0 V}(v_1 v_2; g'^2) \sim (y_2-y_1)^{-2}\,, \qquad (2.19)$$

for large $y_2 - y_1$ and $\underline{B}$ fixed. Actually the rescattering factor $R_{v_0 V}$ is scale invariant in perturbation theory for $d = 4$ transverse dimension and the calculation can proceed by ϵ-expansion. To first order in ϵ we then perform in Eq. (2.18) $\underline{b}$ integration in $d = 4$ and replace the density $\rho^{(2)}$ by the bare density $\rho^{o(2)}$ for $d = 4$ which is obtained from Eq. (3.3) with

$$F(v) = \frac{1}{2\pi^2}\,\frac{e^{-\underline{b}^2/y}}{y^2}\,, \qquad (2.20)$$

and analogous form holds for $F_r(v)$. This gives

$$\ln R_{v_0 V} = -\bar{g}_P^2(\epsilon)\int dv_1\, dv_2\, \frac{F(v_1)F(v_2-v_1)F(V-v_1)}{F(V)}\,F_r(v_2-v_1)\,, \qquad (2.21)$$

where $dv = 2d^4\underline{b}\, dy$, and the effective coupling $\bar{g}_P^2(\epsilon)$ will turn out to be of order ϵ. After performing the $\underline{b}$ integration we have

$$\ln R_{v_0 V} \simeq -\frac{\bar{g}_P^2(\epsilon)}{2\pi^2}\left(\frac{r}{1+r}\right)^2 \int_\Delta^Y \frac{dy\,(Y-y)\exp\left[-\frac{B^2}{Y}\,\frac{ry}{(1+r)Y-ry}\right]}{y^2\left(1-\frac{r}{1+r}\,\frac{y}{Y}\right)^2} \qquad (2.22)$$

$$\simeq -\eta\left[\frac{Y}{\Delta} - \ln\frac{Y}{\Delta}\left(1+\frac{r}{1+r}\left(\frac{B^2}{Y}-2\right)\right)\right]\,,$$

where Δ is a low rapidity cut-off which represents our ignorance of the rescattering function in the low-energy region. Introducing (2.22) into (2.17) we get

$$A(\underline{B},Y) \simeq \frac{\beta_A\beta_B}{2\pi\, Y^{1+2(\nu-1)}}\, e^{\left(\delta-\frac{\eta}{\Delta}\right)Y}\left(\frac{Y}{\Delta}\right)^{\eta} e^{-\frac{B^2}{Y}\left[1+(\nu-1)\ln\frac{Y}{\Delta}\right]}\,, \qquad (2.23)$$

$$\nu - 1 = \frac{r}{1+r}\,\eta\,, \quad \eta = \frac{\bar{g}_P^2(\epsilon)}{2\pi^2}\left(\frac{r}{1+r}\right)^2.$$

It is possible at this stage to renormalize the intercept at $\alpha(0) = 1$, provided

$$\delta' = \frac{\eta}{\Delta} - \delta \tag{2.24}$$

can be put equal to zero. Actually this condition involves not only high-energy parameters like η, but also low-energy ones like Δ and the bare intercept $\alpha_0 = 1 + \delta$ which in multiperipheral models depends on the strength of the low-energy kernel. The value of δ' cannot be therefore reliably estimated by the large rapidity rescattering function (2.19), and its vanishing is a dynamical requirement on low-energy interactions.

If we put $\delta' = 0$ the overlap function (2.23) is not simply a Regge pole with $\alpha(0) = 1$, but is consistent with (2.13) in the ϵ-expansion. The actual calculation of η and ν [and $\bar{g}_p^2(\epsilon)$] comes from the condition (2.19) that the exponent of the rescattering factor be scale invariant in d dimension. In order to compute the left-hand side of Eq. (2.19) we need to anticipate from the next section some features of $\rho^{(2)}_{v_0 V}(v_1 v_2)$. To order ϵ we found: (a) the integral of $\rho^{(2)}$ over the impact parameters $\underline{b}_1$ and $\underline{b}_2$ is a constant in rapidity; (b) $\rho^{(2)}$ shrinks as the propagator, i.e., $\langle b_i^2 \rangle \sim y_i^\nu$. On the other hand, in Eq. (2.19), $F_r(v_2 - v_1)$ is shrinking as $\langle (b_2 - b_1)^2 \rangle \sim (y_2 - y_1)$ and gives a constant after its integration over one impact parameter. The other impact parameter integration in d dimension leads to a quantity which, for (a) and (b), scale as $y^{-d/2\nu}$, so that

$$d\frac{\nu}{2} = 2 \quad \rightarrow \quad \nu \simeq \frac{4}{d} \simeq 1 + \epsilon/4 \ . \tag{2.25}$$

The exponent η is related to ν by $\nu = 1 + r/(1+r)\eta$, where r is the ratio of the slope of $\rho^{(2)}$ and the slope of rescattering Pomeron. Since $\nu > 1$ in the output Pomeron [or in $\rho^{(2)}$] corresponds to $r \to \infty$, as in Eq. (2.14) we have

$$\eta = \nu - 1 = \epsilon/4 \ . \tag{2.26}$$

Summing up, we have shown that owing to the scaling property (2.19) and subject to the condition $\delta' = 0$, the inelastic scattering amplitude has the approximate form

$$\tilde{A}_{in}(s,t) \simeq \beta_A \beta_B \left(\frac{\ln s}{\Delta}\right)^\eta e^{\alpha' t (\ln s)^\nu} \ , \tag{2.27}$$

corresponding to a growing, but factorized, cross-section

$$\sigma_{in}(s) \simeq \beta_A \beta_B \left(\frac{\ell n\, s}{\Delta}\right)^{\eta} . \tag{2.28}$$

The differential cross-section has a forward peak shrinking like $(\ell n\ s)^{\nu}$, and the contribution of $\tilde{A}_{in}$ to the elastic cross-section is

$$\sigma_{el}(s) \simeq \frac{\sigma_{in}^2}{\gamma^{\nu \frac{d}{2}}} \sim (\ell n\, s)^{-p} , \quad p = 2 - \frac{\varepsilon}{2} + O(\varepsilon^2) . \tag{2.29}$$

3. INCLUSIVE DISTRIBUTIONS AND FORM OF PRODUCTION CROSS-SECTIONS

The approximate calculation presented before gives -- to leading order in the ε-expansion -- the absorbed amplitude $A(\underline{B},Y)$ corresponding to purely inelastic events. Here we will generalize the arguments by giving absorptive corrections for higher-order scattering amplitudes, which are relevant for calculating Pomeron vertices, and -- by Mueller diagrams -- the inclusive distributions.

3.1 Vertex corrections

We discuss here the vertex function (Fig. 10) occurring in the absorptive corrections to the purely inelastic overlap function. In the iterative approach (unrenormalized rescattering Pomeron), this vertex is simply defined by

$$\left.\frac{\delta\, G_{v_0 V}(\psi)}{\delta \psi(v)}\right|_{\psi=0} = \int dv'\, dv''\, A(v'-v_0)\, \Gamma(v' v v'')\, A(v-v'') . \tag{3.1}$$

The $3\mathbb{P}$ coupling measured in inclusive experiments is instead defined and discussed in Section 4.

It is possible to rewrite (3.1) in a form which allows the definition of a rescattering factor for the vertex by using the identities

$$\begin{aligned} \frac{\delta}{\delta\psi(v)} K &= K \exp\left[-g^2 \int dv'\, A(v'-v)\,(1+\psi(v'))\frac{\delta}{\delta\psi(v')}\right] \frac{\delta}{\delta\psi(v)} , \\ \frac{\delta}{\delta\psi(v)} G^{(0)}_{v_0 V}(\psi) &= G^{(0)}_{v_0 v}(\psi)\; G^{(0)}_{v V}(\psi) , \end{aligned} \tag{3.2}$$

where K is defined in Eq. (2.5).

In fact, substituting (3.2) into (3.1) we get

$$\frac{\delta}{\delta\psi(v)} G_{v_0 V}(\psi) = K \exp\left[-g^2 \int dv' A(v-v')(1+\psi') \frac{\delta}{\delta\psi'}\right] G^{(0)}_{v_0 v}(\psi) G^{(0)}_{vV}(\psi) \tag{3.3}$$

$$= \exp\left[-g^2 \int dv_1 dv_2 A_{12} (1+\psi_1)(1+\psi_2) \frac{\delta^2}{\delta\psi_1 \delta\psi_2}\right] G_{v_0 V}\left(\psi_1 - g^2(1+\psi_1)A(v_1-v)\right) G_{vV}\left(\psi_2 - g^2(1+\psi_2)A(v_2-v)\right).$$

In other words, the absorptive corrections acting across the vertex can be separated from those giving a propagator renormalization. Calculating (3.3) to the leading order in the ε-expansion, we get

$$\frac{\delta}{\delta\psi(v)} G_{v_0 V}(\psi)\Big|_{\psi=0} \simeq A(v-v_0)\, A(V-v)\, R_{v_0 v V}\,, \tag{3.4}$$

where

$$\ln R_{v_0 v V} = -\frac{\bar{g}_I^2(\varepsilon)}{G^2}\left[\int dv_1 dv_2\, \rho^{0(1)}_{v_0 v}(v_1)\, \rho^{0(1)}_{vV}(v_2)\, F_r(v_2-v_1) + \right. \tag{3.5}$$

$$\left. + \int dv'\, F_r(v'-v)\left(\rho^{0(1)}_{v_0 v}(v') + \rho^{0(1)}_{vV}(v')\right)\right],$$

is the vertex rescattering factor. The various terms in (3.4) correspond, respectively, to Figs. 11a-c. Asymptotically, only the first one survives, because the others scale (for $d = 4$) like Y^{-1} *). One has therefore, after performing the $\underline{b}$ integrations

$$\ln R_{v_0 v V} \simeq -\eta (Y-y) y \int_0^1 dx_1 \int_0^1 dx_2\, \frac{e^{-\frac{r}{1+r}\frac{\left[\underline{b}(1-x_1)+(1-x_2)(\underline{B}-\underline{b})\right]^2}{y(1-x_1)+(Y-y)(1-x_2)}}}{\left[y(1-x_1)+(Y-y)(1-x_2)\right]^2} \tag{3.6}$$

$$\simeq -\eta \ln \frac{(Y-y)y}{Y\Delta'}\,,$$

*) If one calculates (3.5) with renormalized quantities, it is possible that for proper values of d, η, ν, these terms are still scale invariant, and not negligible. This happens, e.g., for pure pole exchange for $d = 2$. Enhanced multiple rescattering corrections can then be calculated as in Ref. 12) and give an alternative mechanism of consistency with unitarity [see also Ref. 13)].

where Δ' is a low rapidity cut-off, of meaning similar to Δ [cf. Eq. (2.22)]. The vertex rescattering factor is therefore approximately given by

$$R_{v_0vV} \simeq \left(\frac{y(Y-y)}{Y\Delta'}\right)^{-\gamma} \quad , \gamma \simeq \eta \simeq \frac{\bar{g}_P^2(\epsilon)}{2\pi^2} \tag{3.7}$$

In momentum space, the behaviour of $\tilde{\Gamma}(\omega_1,\underline{k}_1;\omega_2,\underline{k}_2)$ can be obtained from (3.1) and (3.7) by a Fourier-Laplace transform. For instance, at $\underline{k}_1 = \underline{k}_2 = 0$, one has

$$\tilde{\Gamma}(\omega_1,0;\omega_2,0) = g_P^{(0)2}\,\Gamma(1+\eta)\,\omega_1^{1+\eta}\,\omega_2^{1+\eta}\int dy_1\,dy_2\; y_1^{\eta}\,y_2^{\eta}\; e^{-\omega_1 y_1-\omega_2 y_2} \tag{3.8}$$

$$\times\left[\frac{y_1y_2}{(y_1+y_2)\Delta'}\right]^{-\gamma} \simeq g_P^{(0)}\,(\Delta')^{\gamma}\,\frac{\Gamma(1+\eta)}{\Gamma(1+\eta-\gamma)}\left[\omega_1^{\gamma}+\omega_2^{\gamma}\right] .$$

The vanishing of Eq. (3.8) at $\omega_1=\omega_2=0$ or, in other words, the large y,Y behaviour of the rescattering factor (3.7) means that the effective rescattering interaction is softened, as required by (2.19). Recall, however, that the absorptive vertex function (3.1) is physically different from the diffractive one (Section 4), and is also automatically on the "energy shell" $(\omega=\omega_1+\omega_2)$. One cannot therefore infer from (3.8) the vanishing of the physical $3\mathbb{P}$ vertex which is off energy shell, but with $\omega_i \simeq -\underline{k}_i^2$.

Note also that in our iterative approach, $\gamma \simeq \eta$ by (3.7). This comes from the ratio 1:1 of absorptive corrections to the vertex (Fig. 11a) and to the propagator (Fig. 9a) coming from two-body rescattering. If, however, the rescattering Pomeron is allowed to couple to other Pomerons, giving rise to many-body rescattering (Fig. 12), the value of γ will be modified by additional vertex corrections. An example in which this happens is the RFT (cf. Section 5).

3.2 Inclusive distributions

The generating functional $G_{v_0V}(\psi)$ directly gives [Eq. (2.9)] the inclusive n-particle densities $\rho^{(n)}_{v_0V}(v_1 \ldots v_n)$, in impact parameter, rapidity space. Experimentally, however, one measures transverse momentum distributions, and these are given in terms of off-diagonal matrix elements in impact parameter space which cannot be calculated from $G(\psi)$ alone. For simplicity, we compute therefore from (2.9) the integrated distributions

$$\rho_{\gamma}^{(n)}(y_1 \cdots y_n) = \sigma_{in}^{-1}(Y) \int 2d\underline{B}\, d\underline{b}_1 \cdots d\underline{b}_n\, A(V-v_0)\, \rho_{v_0V}^{(n)}(v_1 \cdots v_n)\,, \tag{3.9}$$

which are basis independent and observable *).

The single particle density is by (2.9)

$$\rho_{v_0V}^{(1)}(v) = \frac{1}{A(V-v_0)} \frac{\delta G_{v_0V}(\psi)}{\delta \psi(v)}\Big|_{\psi=0} \tag{3.10}$$

and is therefore simply related to the vertex function (3.1). Note that this connection holds for two-body rescattering, but breaks down for many-body interactions, because a Pomeron vertex is in that case not necessarily associated with emission of a particle. From Eq. (3.10) we have, to order ϵ

$$\rho_{v_0V}^{(1)}(v) = \frac{A(v-v_0)\,A(V-v)}{A(V-v_0)}\, R'_{v_0vV}$$

$$\simeq \rho_{v_0V}^{0(1)}(v)\Big[1 - \bar{g}_P^2(s)\int dv'dv''\, F_r(v'-v'')\,\frac{1}{G^2} \tag{3.11}$$

$$\times\left(\rho_{v_0v}^{0(2)}(v'v'') + \rho_{vV}^{0(2)}(v'v'') - \rho_{v_0V}^{0(2)}(v'v'') - \rho_{v_0v}^{0(1)}(v')\,\rho_{vV}^{0(1)}(v'')\right)\Big]\,,$$

where we have neglected the corrections of Figs. 13b and c which are not of leading order. The rescattering factor R'_{v_0vV} for inclusive distribution is given by the same form of the vertex rescattering factor R_{v_0vV} in Eq. (3.6). However, while in a full self-consistent solution, as explained, we expect that this last vertex R_{v_0vV} will have in general $\gamma \neq \eta$, for the inclusive vertex R'_{v_0vV} the exponent γ still remains $\gamma = \eta$, to order ϵ. The modification to order ϵ of the $\underline{b}$ distribution in $\rho^{(1)}$ due to the renormaliz ed propagator is of the form $(\nu - 1)\,\ell n\, y$ [cf. Eq. (2.23)], while the one corresponding to R'_{v_0vV} is, for Eq. (3.6), of order η (constant in y). The $\rho^{(1)}$ distribution shrinks then in b as the propagator $\langle b^2 \rangle \sim y$.

*) The effects of absorption on momentum distributions are likely to be important and deserve further study. We discuss this point for the triple Regge region (Section 4).

Equation (3.11) can be cast also in the form

$$\rho^{(1)}_{v_0V}(v) \simeq \rho^{o(1)}_{v_0V}(v) - \bar{g}^2_{\underline{b}}(\varepsilon) \int dv' dv'' F_r(v'-v'') \frac{1}{G^2} \left(\rho^{o(3)}_{v_0V}(v'v''v) - \rho^{o(1)}_{v_0V}(v) \rho^{o(2)}_{v_0V}(v'v'') \right) \quad (3.12)$$

in agreement with Eq. (3.10). After $\underline{b}$ integration we obtain, from Eq. (3.4)

$$\rho^{(1)}_Y(y) \simeq G - \bar{g}^2_{\underline{b}}(\varepsilon) \int \frac{dy' dy''}{(y''-y')^2} \frac{1}{G^2} \left[\rho^{o(3)}_Y(y'y''y) - G \rho^{o(2)}_Y(y'y'') \right], \quad (3.13)$$

where $\Delta < y'' - y' < Y$, and Δ is the low rapidity cut-off for the rescattering function $F_r(v'' - v')$ [cf. Eq. (2.22)]. On the other hand, for large $y'' - y'$ the integrand vanishes, due to Eq. (3.4), so that one has

$$\rho^{(1)}_Y(y) \simeq G(1 - \eta K_1) . \quad (3.14)$$

The precise value of the constant K_1 is dependent on short-range order physics and therefore not specified in our model, or in other words, cut-off dependent. In fact, by subdividing the integration region according to whether $y', y'' \leq y$ or $y' < y < y''$, we get

$$K_1 \simeq \ln \frac{\Delta}{\Delta'} \quad (3.15)$$

where Δ' is the cut-off which parametrizes $\rho^{o(3)}$ accross the vertex $[\theta(y'' - y' - \Delta')]$. From (3.16) it appears that the rapidity dependent terms cancel, but not in general the cut-off dependent constants. In exponentiated form (3.13) becomes

$$\rho^{(1)}_Y(y) \simeq G \left(\frac{y(Y-y)}{Y\Delta} \right)^{\eta} R'_{oyY} \simeq G \left(\frac{\Delta'}{\Delta} \right)^{\eta} . \quad (3.16)$$

We then see that after $\underline{b}$ integration, the growth of the Pomeron propagator is compensated by the screening of the rescattering factor R'_{oyY} to give a constant plateau as for the bare distribution; absorption only modifies the value of the plateau.

Both Eqs. (3.11) and (3.12) are simply generalized to higher-order distributions by application of (3.9) and (3.2). For two particles we have

$$\rho^{(2)}_{\nu_0 V}(\nu_1\nu_2) = \frac{A(\nu_1)\,A(\nu_2-\nu_1)\,A(V-\nu_2)}{A(V)}\; R'_{\nu_0\nu_1\nu_2}\; R'_{\nu_1\nu_2 V}\; R'_{\nu_0\nu_1\nu_2 V}\,, \tag{3.17}$$

where the two-interval rescattering factor is given by

$$\ln R'_{\nu_0\nu_1\nu_2 V} = -\,\bar{g}_p^{\,2}(\varepsilon)\int d\nu'\,d\nu''\,F_r(\nu'-\nu'')\,\frac{\rho^{o(1)}_{\nu_0\nu_1}(\nu')\,\rho^{o(1)}_{\nu_2 V}(\nu'')}{G^2}\,. \tag{3.18}$$

The b dependence of $\rho^{(2)}$ can be deduced, to order ε, as for the case of $\rho^{(1)}$, and we found that it shrinks as the propagator, i.e., $\langle b_i^2\rangle \sim y_i^{\nu}$. To leading order in ε we get

$$\rho^{(2)}_{\nu_0 V}(\nu_1\nu_2) \simeq \rho^{o(2)}_{\nu_0 V}(\nu_1\nu_2) - \bar{g}_p^{\,2}(\varepsilon)\int d\nu'\,d\nu''\,F_r(\nu'-\nu'')\,\frac{1}{G^2}\left[\rho^{(4)}_{\nu_0 V}(\nu'\nu''\nu_1\nu_2) - \rho^{(2)}_{\nu_0 V}(\nu_1\nu_2)\,\rho^{(2)}_{\nu_2 V}(\nu'\nu'')\right], \tag{3.19}$$

and after $\underline{b}_1$, $\underline{b}_2$ integrations

$$\rho^{(2)}_{Y}(y_1y_2) \simeq G^2 - \bar{g}_p^{\,2}(\varepsilon)\int \frac{dy'\,dy''}{(y''-y')^2}\,\frac{1}{G^2}\left[\rho^{(4)}_{Y}(y'y''y_1y_2) - \rho^{(2)}_{Y}(y_1y_2)\,\rho^{(2)}_{Y}(y'y'')\right], \tag{3.20}$$

where $\Delta < y'' - y' < Y$ and the integrand vanishes for large rapidity differences. A simple calculation shows that, for $y_2 - y_1 \gg \Delta$

$$\rho^{(2)}_{Y}(y_1y_2) \simeq G^2(1-2\eta k_1) \simeq \left[\rho^{(1)}_{Y}\right]^2, \tag{3.21}$$

and correlations are asymptotically vanishing. Actually, correlation function can be directly computed from Eqs. (3.13) and (3.20), and we found

$$C^{(2)}_{Y}(y_1y_2) \equiv \rho^{(2)}_{Y}(y_1y_2) - \rho^{(1)}_{Y}(y_1)\,\rho^{(1)}_{Y}(y_2) \simeq$$

$$\simeq \bar{g}_p^{\,2}(\varepsilon)\int \frac{dy'\,dy''}{(y''-y')^2}\; C^{o(4)}_{Y}(y_1y_2y'y'') \simeq -\eta\,G^2 K_2(y_2-y_1)\,, \tag{3.22}$$

which is dependent on short-range order dynamics and asymptotically vanishing.

The results (3.16), (3.21) and (3.22) mean that after absorption one still has a basically short-range order production mechanism, with logarithmic multiplicity and finite, small corrections to correlation functions. Correlations decreasing as inverse powers of $y_2 - y_1$ are not excluded, and in fact come from multiple rescattering also. However, the integrated correlations should, by (3.23), increase not faster than $\ell n\, s$. A confirmation of these results (giving all correlation moments increasing as $\ell n\, s$ only) comes from the evaluation of the absorptive corrections to the individual σ_N given next.

3.3 Form of partial cross-section σ_N

The previous result that after absorption the production is still of short-range type can be directly derived also from the study of production cross-sections. Instead of computing σ_N by the present formalism from $G(\psi)$, we prefer here to show the calculation for a naive, but perhaps more intuitive model in which the bare production amplitudes are simply

$$\left| A_N^{(0)}(v_0 v_1 \dots v_N V) \right|^2 = G^N \prod_{i=1}^{N} f\left((\underline{b}_i - \underline{b}_{i-1})^2\right) \vartheta(y_i - y_{i-1})\, e^{-(G-\delta)Y} \qquad (3.23)$$

where $f(B^2)$ is a normalized distribution for which $\langle B^2 \rangle \simeq \alpha'/G$.

In order to compute the absorptive effects, we take from Eq. (2.19) the result that the effective rescattering interaction, after $\underline{b}$ integrations, behaves as $\bar{g}_P^2/y^2$ for large rapidity differences. We then calculate the cross-sections' rescattering factor

$$R_{N,Y} = \left\langle \exp\left(- \sum_{i>j} A_{eff}(y_i - y_j) \right) \right\rangle_N , \qquad (3.24)$$

by averaging over the distribution (3.23). A simple calculation shows that

$$\left\langle \frac{1}{(y_i - y_j)^2} \right\rangle_N = \frac{N(N-1)}{k(k-1)} \frac{1}{Y^2} , \quad (k = i-j) \qquad (3.25)$$

We therefore replace y_i in (3.24) by the average rapidity $\langle y_i \rangle_N = iY/N$, to get

$$\ell n\, R_{N,Y} \simeq - \bar{g}_P^2 \frac{N^2}{Y^2} \sum_k \frac{N-k}{k^2} \simeq - \bar{g}_P^2 N \rho^2 \left[a - \frac{\ell n N}{N} + O\left(\frac{1}{N}\right) \right] ,$$

$$\rho \equiv \frac{N}{Y} , \quad a = \sum \frac{1}{k^2} . \qquad (3.26)$$

It is now a straightforward matter to calculate from Eqs. (3.23) and (3.26) both the renormalized density ρ and the generating function. We have in fact

$$\sigma_N \simeq e^{(\delta-G)Y} \frac{(GY)^N}{N!} R_{N,Y} \simeq e^{(\delta-G)Y + \phi(N,Y)} ,$$

$$\phi(N,Y) = N \ln GY - N(\ln N - 1) - \bar{g}_P^2 \frac{N^3}{Y^2} \left(a - \frac{\ln N}{N} \right) + O(1) . \tag{3.27}$$

By the stationary phase method we get

$$\ln \frac{G}{\rho} = 3 \bar{g}_P^2 \rho^3 , \quad \rho \simeq G (1 - 3a \bar{g}_P^2 G^2) , \tag{3.28}$$

to be compared with (3.19). [The parameter a corresponding to K_1 is still unknown because (3.26) is valid only for $y_j - y_i > \Delta$, or $k > \Delta\rho$.] Moreover, we get

$$\ln \sigma_{in} \simeq Y \left(\delta - G + \rho + 2a \bar{g}_P^2 \rho^3 \right) + \rho^2 \bar{g}_P^2 \ln \rho Y \tag{3.29}$$

which fixes δ' and η, consistently with Eqs. (2.22) and (2.24).

This approach makes it clear that the generating function has the short-range order form

$$\ln Q(z) = Y (\rho(z) - \rho) \left[1 + 2a \bar{g}_P^2 \left(\rho^2(z) + \rho(z)\rho + \rho^2 \right) \right] ,$$

$$\rho(z) = Gz \left(1 - 3a \bar{g}_P^2 G^2 z^2 \right) . \tag{3.30}$$

This result is similar to that obtained by Arnold and Steinhoff [19] in a one-dimensional fluid model with attractive nearest-neighbour forces and repulsive long-range interactions. The main differences are that:

i) The exponent of R_{NY} behaves essentially as N^3/Y^2, instead of N^2/Y. This is typical of the $1/y^2$ repulsive interaction due to absorption through the Pomeron itself.

ii) There is an additional $N^2/Y^2 \ln N$ piece which gives σ_{in} the factor $(\ln s)^\eta$: this is the source of the critical exponents.

Note that any rescattering interaction which has a local asymptotic part y^{-p} $(p>1)$ will give rise to logarithmic multiplicities. This confirms the expectation that the cancellation proved in (3.16) to lowest order in ϵ is indeed a general feature.

Note finally that a $\underline{B}$ dependent rescattering factor can also be computed and used for studying σ_{NB_2} and shrinkage properties. In fact, from (3.23) one can show that, if $\langle \underline{B}_i \rangle = \alpha'/G$ and $r = \alpha'/\alpha'_0$, then

$$\left\langle \frac{\exp\left(-r\,\frac{(\underline{b}_j-\underline{b}_i)^2}{y_j-y_i}\right)}{(y_j-y_i)^2} \right\rangle_N \simeq \frac{N^2}{Y^2}\,\frac{1}{k^2}\,\frac{\exp -\left(G\,\frac{B^2}{N}\,\frac{k}{N}\,\frac{r}{1+r}\right)\Big/\left(1-\frac{k}{N}\,\frac{r}{1+r}\right)}{\left(1-\frac{k}{N}\,\frac{r}{1+r}\right)}\,. \tag{3.31}$$

From (3.31) the result (2.23) can be rederived.

4. ABSORPTION FOR DIFFRACTIVE EVENTS

Let us illustrate the absorptive model for the case where a single large mass is diffractively excited. The bare production amplitude is described in Fig. 14a where a bare Pomeron is exchanged so that particles are produced with a rapidity gap $0 - y$. Absorption for this Pomeron takes place as described in Section 2. All produced particles in the range $v - V$ are assumed to rescatter not only among themselves, but also with intermediate states of exchanged bare Pomeron as described in Fig. 14b. The overlap function for these events is simply given in terms of the absorbed functional $G(\psi)$ by

$$g_P^{(0)} \exp\left\{-gg'\int \frac{\delta}{\delta\varphi(v)}\,F_r(v-v')\left(\frac{\delta}{\delta\varphi_1(v')}+\frac{\delta}{\delta\varphi_2(v')}\right)dv\,dv'\right\}\frac{1}{G^{3/2}}\,G_{v_0V}(\psi_1)G_{v_0V}(\psi_2)G_{vV}(\psi), \tag{4.1}$$

where $\psi(u) = e^{\varphi(v)} - 1$, etc. Graphs contributing to the overlap function are represented in Fig. 15. Note that in Eq. (4.1) we have introduced, in addition to the coupling gG (Fig. 16a) and $g_P^{(0)} = gG$ (Fig. 16b), the coupling g' related to the vertex in Fig. 16c involving no cut Pomerons. As mentioned in subsection 3.1, the latter can give rise to many-body rescattering in the final state. Recall, however, that for the single fireball it would modify the value of critical index γ for the absorbed vertex function R_{v_0vV} but not the one of the inclusive vertex correction R'_{v_0vV}, at least to order ϵ.

The leading particle inclusive distribution for these events can be obtained from Eq. (4.1) by an impact parameter displacement, and we have

$$\rho_Y(y,q^2) = \frac{1}{\sigma_{in}(Y)} \frac{d\sigma}{dy\, d\underline{q}} = \int \frac{d\underline{b}'}{(2\pi)^2} e^{i\underline{b}'\underline{q}} \; 2\, d\underline{b}\; d\underline{B}\; M(v_1 v_2 v V), \tag{4.2}$$

where $v_1 = (0, \underline{b}'/2)$, $v_2 = (0, -\underline{b}'/2)$, $v = (y, \underline{b})$, and $V = (Y, \underline{B})$. $M(v_1 v_2 v V)$ is the three-Pomeron Mueller amplitude (Fig. 17) in the impact parameter space and to order ϵ is given by

$$M(v_1 v_2 v V) = g_P^{(0)} \exp\left[-gg' \int \frac{\delta}{\delta\varphi} F_r\left(\frac{\delta}{\delta\varphi_1} + \frac{\delta}{\delta\varphi_2}\right)\right] \frac{1}{G^{3/2}} G_{v_1 V}(\varphi_1)\, G_{v_2 V}(\varphi_2)\, G_{vV}(\varphi) \tag{4.3}$$

$$\simeq \frac{g_P^{(0)}}{G^{3/2}} A(v-v_1) A(v-v_2) A(V-v)\, \tilde{R}_{v_1 V}\, \tilde{R}_{v_2 V} .$$

The rescattering factors $\tilde{R}$ have the same form as the vertex rescattering factor R computed in Section 3 [Eq. (3.6)] but, in general, with a different index that we call $\gamma'/2$. It is possible that $\gamma' = \gamma$, but as discussed in subsection 5.2, we cannot prove it at this level.

The y-distribution ($y \approx \ell n\, s/M^2$, M missing mass) is obtained from Eqs. (4.2) and (4.3)

$$\rho_Y(y) = \frac{1}{\sigma_{in}} \frac{d\sigma}{dy} \simeq g_P^{(0)} \frac{1}{\sigma_{in}(Y)} \int d\underline{b}\; 2\, d\underline{B}\; \frac{A^2(v) A(V-v)}{G^{3/2}}\, \tilde{R}^2_{ovV} . \tag{4.4}$$

From the asymptotic form of the vertex correction R [Eq. (3.7)] we have, to order ϵ

$$\rho_Y(y) \approx \beta_A\, g_P^{(0)}\, \frac{\sigma_{el}(y)}{G^2}\, \frac{\sigma_{in}(Y-y)}{\sigma_{in}(Y)} \left(\frac{y(Y-y)}{Y\Delta'}\right)^{-\gamma'},$$

$$\approx \beta_A\, \frac{\sigma_{el}(y)}{G^2}\, g_P^{(0)} \left(y/\Delta'\right)^{-\gamma'} \left(\frac{Y-y}{Y}\right)^{\eta-\gamma'}, \tag{4.5}$$

$$\sim y^{-\beta-\gamma'}, \quad \beta = 2 - \frac{\epsilon}{2} + O(\epsilon^2) .$$

We see here that the vertex correction compensates the increase at large rapidities of renormalized propagator giving a y-distribution decreasing faster than y^{-1}, and therefore consistent with unitarity.

Besides this general result, similar to RFT [9], our explicit model gives also the y, q^2-distribution from Eq. (4.2), by including also the b dependence of rescattering factors. A remarkable fact is that, due to the positivity of the quantity in Eq. (4.2) for all impact parameters, the q^2-distribution is decreasing away from $q^2 = 0$, i.e., cannot have any turnover. The distribution can be explicitly computed by observing that

$$A(\nu-\nu_1)A(\nu-\nu_2) \approx A^2(\nu)\, e^{-b'^2/2y^\nu}, \tag{4.6}$$

and, from Eq. (3.6)

$$\tilde{R}_{\nu_1 \nu V}\, \tilde{R}_{\nu_2 \nu V} \approx \left(\tilde{R}_{o\nu V}\right)^2 e^{\frac{b'^2}{2y}\frac{\gamma'}{4}}. \tag{4.7}$$

From Eqs. (4.2) and (4.4) we have

$$\rho_Y(y,q^2) \approx \rho_Y(y)\, e^{-q^2 B(y)}/B(y) \tag{4.8}$$

with

$$B(y) \simeq 2\alpha' y/\left(1 - \frac{\gamma'}{4} + (\nu-1)\ln y\right) \approx 2\alpha'\left(1+\frac{\gamma'}{4}\right) y^\nu. \tag{4.9}$$

The q^2-distribution in this model has a peak at $q^2 = 0$ with a slope $B(y)$ sharper than the one of $d\sigma_{el}/dt$ (i.e., $2\alpha' y^\nu$). This result is consistent with the expected widening of the distribution at large q^2. The consistency of $\rho_Y(y,q^2)$ with unitarity in this model is then achieved not by a turnover or a zero at $q^2 = 0$, but by the vanishing, faster than y^{-1}, of the distribution at large y, due to the vertex screening.

Screening effects are also present in multiple diffractive events (Fig. 18). Here there are two important phase space regions: (a) the Finkelstein-Kajantie region where all produced particles are largely separated in rapidity; the size of the gaps $\Delta_i = y_i - y_i'$ are much larger than the size of fireballs $y_i - y'_{i-1}$. Here a Regge pole $\alpha(0) = 1$ violates unitarity, and rescattering corrections among produced particles are not sufficient to enforce it [14]. However, vertex corrections from intermediate state rescattering arise as in Eq. (4.1) and reduce the probability $p(\Delta_i)$ for a gap Δ_i as in Eq. (4.4). The resulting contribution to σ_{tot} is therefore finite and small [9], consistently with s-channel unitarity; (b) the phase space region where the gap size Δ_i is much larger than the fireball size $(1 \ll \Delta_i \ll y_1 - y_{i-1})$, which gives the main contribution to σ_{tot}. Noting that the probability of having the gap Δ_i at y_i is proportional to $\rho_Y^{(n)}(y_1, y_2 \ldots y_n)$, we can use the results of Section 3 to get

$$\frac{d\sigma}{\pi dy_i d\Delta_i} \propto \sigma_{in}(Y)\, g_p^{(0)2n} \prod_i \vartheta(y_i - y_{i-1})\, p(\Delta_i)\, \Delta_i^{\gamma-\gamma'}, \qquad (4.10)$$

$$p(\Delta) \sim \Delta^{-\beta-\gamma'}, \quad (\Delta_i << y_i - y_{i-1}),$$

where $\sigma_{in}(Y)$ is the single fireball cross-section, and we have identified the cut-off Δ' occurring in Eq. (3.17) with the proper value of the gap. It is straightforward to see that Eq. (4.10) gives a small positive intercept renormalization. In fact, the n-gap cross-section is

$$\sigma_n(Y) \approx \sigma_{in}(Y) \frac{(\delta' Y)^n}{n!}, \quad \delta' \propto g_p^{(0)2} \int d\Delta\, p(\Delta)\, \Delta^{\gamma-\gamma'}. \qquad (4.11)$$

It is possible at this stage to renormalize the intercept at $\alpha(0) = 1$ for the sum of all σ_n, provided that δ' in Eq. (2.24) is given by the value in Eq. (4.11). This implies then that the single fireball amplitude in Eq. (2.23) is damped at large Y by a factor $e^{-\delta' Y}$, so that the cross-section in Eq. (2.28) is increasing up to a rapidity $Y_0 \simeq \eta/\delta'$ and then exponentially decreasing.

5. SUMMARY AND DISCUSSION

The general outcome of the absorptive model that we have presented is that s-channel unitarity essentially affects the total cross-sections (the logarithmic increase is the reminder of $\alpha_0 > 1$) but not strongly the multiplicity distribution. If one thinks of the multiperipheral model more as a phenomenological tool than as a theory, we see that it has only to be supplemented by some conditions on Pomeron vertices and factorization assumptions. We now explain in more detail what we have obtained.

5.1 Summary of results

1) The inelastic cross-sections are factorized and asymptotically growing with s as $\sigma_{in}(s) \approx \beta_A \beta_B (\ell n\, s/\Delta)^{\eta}$. The slope $B(s)$ of the elastic differential cross-section is shrinking with s as $B(s) \approx B_0 + 2\alpha'(\ell n\, s)^{\nu}$. The elastic cross-section is then finally decreasing as $\sigma_{el} \approx \sigma_{in}^2/B$. The critical exponents η, ν have been computed to order ϵ for purely inelastic events in the iterative approach and one gets $\eta \simeq \nu - 1 \simeq \epsilon/4$.

2) The Pomeron vertices are screened at large rapidities. The screening is characterized by a critical index γ which in the iterative approach to the single fireball, is to order ϵ, $\gamma \simeq \eta$. The features of this solution

are similar in this respect to the RFT [9),10)], but with different values of the critical indices (see below).

3) The average multiplicity is growing as $\ell n\ s$, and only integrable correlations are introduced by absorption. These features can be understood both in an inclusive and exclusive way. (a) From the study of inclusive $\rho^{(n)}$ distributions we have shown that there is a general compensation between the screening of the inclusive vertices and the growing of cross-sections. The $\rho^{(n)}$ distributions are therefore still factorized [$\rho^{(n)} \simeq (\rho^{(1)})^n$] for large rapidity differences, so that no large-range correlations are present to leading order in $\ell n\ s$. (b) From the study of production cross-sections $\sigma_N(s)$, we have shown that the effect of long-range repulsive interactions (absorption) leads essentially to an intercept renormalization with a critical behaviour $(\ell n\ s)^\eta$ for the total cross-section. It is still possible, however, to define a pressure for the generating function [Eq. (3.31)], so that only integrable correlations are present.

4) The triple Pomeron Mueller amplitude, relevant for the diffractive production of a single large mass M, is in the impact parameter representation positive definite. This fact entails that the consistency with unitarity of the leading particle inclusive cross-section is achieved in our model by the screening in the large rapidity region of the three-Pomeron vertex, and not by a zero or turnover of the distribution at $q^2 = 0$.

5) This same mechanism (screening of Pomeron vertices for large rapidities) makes the Finkelstein-Kajentie region (where all produced particles are largely separated in rapidity) also consistent with unitarity. When all the possible diffractive events are taken into account (fireball expansion), a small modification of the intercept renormalization for the single fireball amplitude has to be considered.

As emphasized in Ref. 9), the relevance of these results at present energies is dependent on the value of the bare coupling g_P^o. In fact, the perturbation expansion parameter is $g_P^o/\alpha'\ Y$, so that we expect that the transition region cut-off is $\bar{Y} \simeq \alpha'/g_P^o$. The simplest possibility [9)] is just the triple-Pomeron coupling $g_P(0,0,0)$ measured in diffractive excitation. In this case $\bar{Y} \simeq 20\text{-}40$, according to the various estimate [20)], so that only perturbation expansion is relevant at ISR energies, and our results only for ultra-asymptotic consistency.

A different possibility is that g_P^o is much larger than the observed coupling $g_P(0,0,0)$, so that the non-perturbative solution gives at least a sensible parametrization for comparison with experimental data. Despite the fact that the normalization of the triple-Pomeron coupling in the ϵ-expansion $\bar{g}_P(\epsilon)$ is too large, the smallness of the observed value of $g_P(0,0,0)$ should be explained by the screening factor $y^{-\gamma'}$ due to

absorption. It is, in fact, clear that in these formulae $\alpha' y$ should be replaced by $B(y) \simeq B_o + \alpha' y$, and a sizeable value of B_o is anyway needed to make the ratio σ_{el}/σ_{tot}, which results asymptotically decreasing, compatible with present data [1].

An important remark, irrespective of which approach is valid, is that the increase of σ_{tot} cannot be attributed in this model entirely to a single class of events. If one takes the renormalized fireball expansion of Eq. (4.2), it is clear that purely inelastic events (single fireball) increase for a while, and at $Y_o \simeq \eta/\delta$ start to exponentially decrease by unitarity damping. Single diffractive events take then over up to $Y_1 \simeq (\eta + 1)/\delta$ and so on for multiple diffractive events. The phenomenological result [20] that the increase of present data is compatible with the one expected from single diffractive excitation [11], is from this point of view very interesting but dependent on the experimental energy range.

5.2 Comparison with Reggeon field theory

The existence of critical indices η, γ, ν was long ago proposed by Gribov and Migdal [7] for the theory of interacting Pomeron amplitudes, and their values in the ϵ-expansion have recently been given by renormalization group methods [9),10]. Our results are the s-channel counterpart of these approaches.

While RFT are motivated by t-channel discontinuity rules for Reggeons [4], we try to enforce s-channel unitarity from the start, and we are able to specify a definite set of final-state particles and production amplitudes. The advantage of dealing with physical events is paid by the need of building up the Pomeron in an iterative fashion: in fact the absorptive effects come in as soon as the cross-section builds up, and to start with we have to assume the rescattering Pomeron be a pole, while the output is not.

Some peculiar features arise in the s-channel (iterative) approach:

1) There are several triple-Pomeron vertices, not just one. We have defined three (Fig. 16): (a) the absorptive vertex; (b) the diffractive one and; (c) the vertex for Pomeron amplitudes. Since they characterize in our approach different physical processes (e.g., two-body rescattering versus three-body), these couplings are not a priori equal. However, if we believe RFT, they should come out from taking discontinuities of a single vertex function and therefore related to the same coupling constant (see below).

2) The values of η, γ, ν that we find for the single fireball are different from RFT. This is perhaps due to both the lack of complete

self-consistency *), and to the explicit occurrence of only one process (two-body rescattering). We have already mentioned that the introduction of three- and many-body rescattering will modify γ, although not $\rho^{(2)}$ (subsections 3.1 and 3.2).

The problem of the critical indices for various classes of events in a fully self-consistent solution has not yet been solved. Also, it is not clear whether self-consistency is an absolute requirement, since the dynamics might evolve with energy [21]. However, one can better understand what we do by giving a discontinuity rule for Gribov graphs. We take the recipe 1:(-2) for the weight of diffractive versus absorptive discontinuities, since the one of Gribov, Abramovskii and Kancheli [22] contains a different kind of process, the polyperipheral production (Fig. 19) **).

By the discontinuity rule we see (Figs. 20, 21) that a single Gribov graph generates several cut ones. Comparing graphs 20a and 21a (two-body rescattering) with the amplitudes 20α and $21\alpha,\beta$, we see that the counting 4:1 of vertex versus propagator corrections for amplitudes is modified into 1:1 for the two-body rescattering contribution. This explains why $\gamma = \eta$ in the iterative approach [Eq. (3.7)], while $\gamma = 4\eta$ for RFT. The former result will be modified at the single fireball level if we introduce three-body rescattering graphs 21b,c. Graph 21d is instead an absorptive correction to one-gap events, while graph 20b is the related one-gap amplitude.

It is clear therefore that the RFT counting cannot be reproduced without considering together several classes of events, with all vertices having equal couplings. The approach we have followed is the most natural from an s-channel point of view, and might turn out to be the correct one. We do not consider, however, the particular values for the critical indices we have given as very reliable, both because the ε-expansion is poorly convergent [23], and because we need a better understanding of mixed diffractive-absorptive graphs like 21d and their relative couplings. While the physical results we have mentioned are qualitatively independent of the size of η, γ, and ν, a reliable calculation of these and of the rapidity scales Δ that we have introduced, is essential for a comparison with experimental data.

---

*) This should be the origin of the result $\nu = 1 + \eta$ (instead of $\nu = 1 + \frac{1}{2}\eta$ of RFT), because the output Pomeron has an infinite slope with respect to the rescattering one.

**) We understand that the discontinuity rule of Ref. 22) may be in contrast with generalized Steinmann relations (T. Degrand, MIT Preprint).

ACKNOWLEDGEMENTS

We are grateful to many colleagues of CERN Theoretical Study Division for interesting remarks.

REFERENCES

1) See, for example, A. Diddens, Rapporteur's Talk at the XII Int. Conf. on High-Energy Physics, London (1974).

2) K. Wilson, Cornell Preprint CLNS-130;
K. Fialkowski and H. Miettinen, Phys. Letters 43B, 61 (1973);
H. Harari and E. Rabinovici, Phys. Letters 43B, 43 (1973);
L. Van Hove, Phys. Letters 43B, 65 (1973);
W. Frazer, R.D. Peccei, S. Pinsky and C.I. Tan, Phys. Rev. D7, 2647 (1973);
see also, L. Caneschi and M. Ciafaloni, Invited Talk at the Aix-en-Province Conf. on Elementary Particles, Journal de Physique 34, 268 (1973).

3) G.F. Chew, Phys. Rev. D7, 934 (1973).

4) A.R. White, Nuclear Phys. B50, 130 (1972).

5) J. Finkelstein and M. Jacob, Nuovo Cimento 56A, 681 (1968);
L. Caneschi, Phys. Rev. Letters 23, 254 (1969).

6) H. Cheng and T.T. Wu, Phys. Rev. Letters 24, 1456 (1970).

7) J. Finkelstein and F. Zachariasen, Phys. Letters 34B, 631 (1971);
V.N. Gribov, JETP (Sov. Phys.) 26, 414 (1968);
V.N. Gribov and A.A. Migdal, Sov. Journ. Nucl. Phys. 8, 583, 703 (1969).

8) See, for example, L. Caneschi and M. Ciafaloni, Ref. 2).

9) A.A. Migdal, A.M. Polyakov and K.A. Ter-Martirosian, Phys. Letters 48B, 239 (1974); and Moscow Preprint ITEP-102 (1973).

10) H.D.I. Abarbanel and J.B. Bronzan, Phys. Letters 48B, 345 (1974); and FNAL Preprint FNAL-Pub 73/91 THY (1973).

11) D. Amati, L. Caneschi and M. Ciafaloni, Nuclear Phys. B62, 173 (1973).

12) M. Ciafaloni and G. Marchesini, Nuclear Phys. B71, 493 (1974).

13) M. Ciafaloni and G. Marchesini, Invited Paper presented at the XVII Int. Conf. on High-Energy Physics, London (1974).

14) A. Schwimmer, Weizmann Preprint WIS 74/4-Ph. (1974).

15) H.D.I. Abarbanel, Phys. Rev. D6, 2788 (1973);
G.F. Chew, Phys. Rev. D7, 934 (1973).

16) K.G. Wilson, Phys. Rev. Letters 28, 548 (1972); Phys. Rev. D7, 2910 (1973).

17) H.D.I. Abarbanel and R.L. Sugar, FNAL Preprint FNAL-Pub 74/33 THY (1974).

18) M. Ciafaloni and G. Marchesini, Proc. IX Rencontre de Moriond, 1974 (to be published).

19) R.C. Arnold and J. Steinhoff, Phys. Letters 45B, 141 (1973).

20) D.P. Roy and R.G. Roberts, Rutherford Preprint RL-74-022.

21) D. Amati, Phys. Letters 48B, 253 (1974).

22) V.A. Abramovskii, V.N. Gribov and O.V. Kancheli, Proc. XVI Int. Conf. on High-Energy Physics, Vol. 1, p. 389.

23) M. Baker, Phys. Letters 51B, 158 (1974).

FIGURE CAPTIONS

Fig. 1 : Multiperipheral model for the cut bare Pomeron.

Fig. 2 : Diffractive and absorptive corrections to the bare Pomeron. Wavy line represents a Pomeron.

Fig. 3 : Three-Pomeron Mueller graph.

Fig. 4 : Typical elastic rescattering correction to a multiperipheral production amplitude [cf. Eq. (1.5) in the text].

Fig. 5 : Bare Pomeron propagator $G^{o}_{v_o V}(\psi)$ in v-space in presence of an external source $\psi(v)$; $v_i = (\underline{b}_i, y_i)$, $v_o = (\underline{0}, 0)$, $V = (\underline{B}, Y)$.

Fig. 6 : Graphs contributing to the renormalized Pomeron $A(v)$. Any pair of point of cut bare Pomeron are connected by the rescattering function $\ell n\,|S| \simeq -A$.

Fig. 7 : First iteration of the non-linear equation represented in Fig. 6. The rescattering function $\ell n\,|S|$ is approximated by a bare Pomeron.

Fig. 8 : Typical absorptive corrections contributing to $\rho^{(2)}_{v_o V}(v_1 v_2)$ to order g^2.

Fig. 9 : Second-order Gribov graph. g^{o}_{P} is the bare triple-Pomeron coupling.

Fig. 10 : Three-Pomeron vertex function occurring in absorptive corrections to purely inelastic overlap function.

Fig. 11 : Graphical representation of the various terms contributing to order ϵ to the vertex function in Fig. 10 [see Eq. (3.5) in the text].

Fig. 12 : Absorptive corrections due to three-body rescattering.

Fig. 13 : Graphical representation of the various terms to order ϵ contributing to the single-particle distribution $\rho^{(1)}$.

Fig. 14 : Production amplitude for events in which a large mass is diffractively excited:

(a) bare amplitude; (b) absorbed amplitude.

Fig. 15 : Absorptive contribution to the overlap function for events where a large mass is diffractively excited.

Fig. 16 : Three-Pomeron vertices:

(a) vertex occurring in absorptive corrections to the single fireball;

(b) vertex occurring in diffractive events;

(c) vertex occurring in absorptive correction to the diffractive vertex and in multiple rescattering.

Fig. 17 : Three-Pomeron Mueller amplitude in the impact parameter space.

Fig. 18 : Multiple diffractive events.

Fig. 19 : Polyperipheral production graph.

Fig. 20 : (α) Second-order Gribov graph for Pomeron propagator;

(a)(b) Discontinuity contributions to the second-order graph, according to the rules in the text.

Fig. 21 : (α,β)(a) Second-order Gribov graph for three-Pomeron vertex;
(a)(b)(c)(d) Discontinuity contributions to the vertex, according to the rules in the text.

1

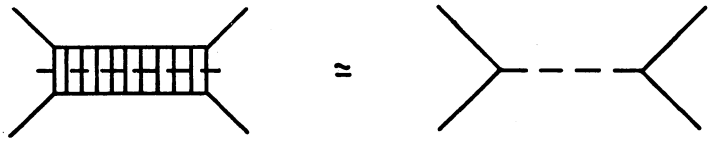

2

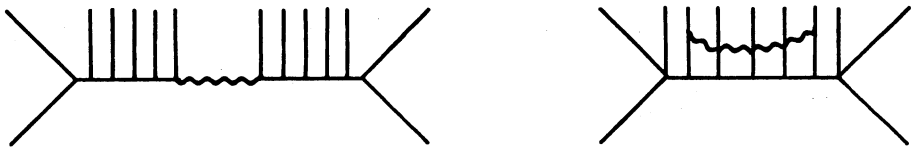

3

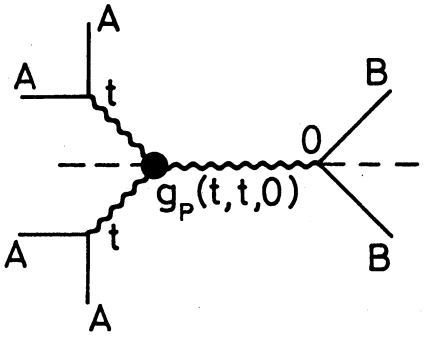
A
A
t
B
0
$g_p(t,t,0)$
t
A
B
A

4

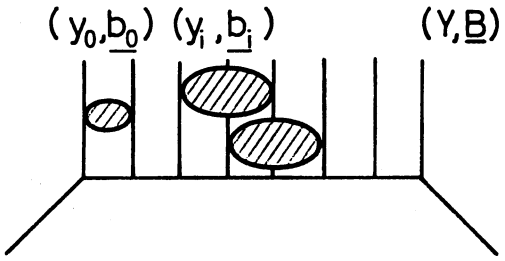
$(y_0,\underline{b}_0)$
$(y_i,\underline{b}_i)$
$(Y,\underline{B})$

5

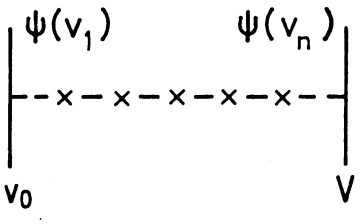
$\psi(v_1)$
$\psi(v_n)$
v_0
V

6

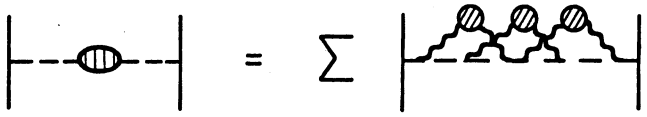
=
$\sum$

7

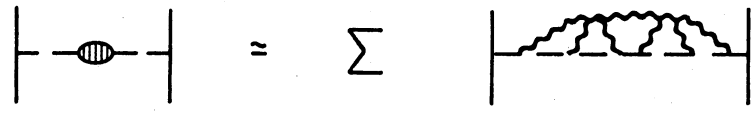

8

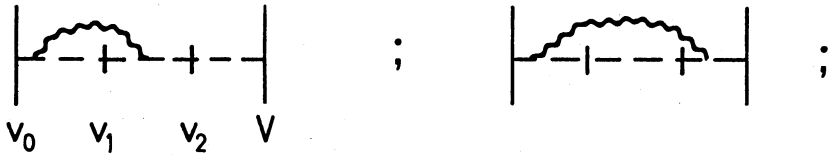

a ; b ;

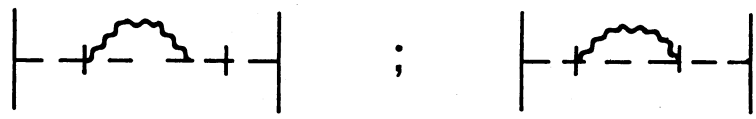

c ; d

9

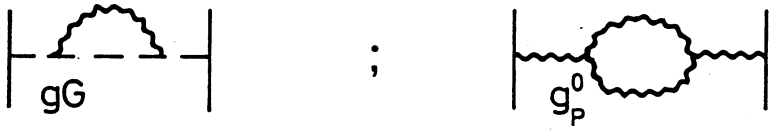

a ;

10

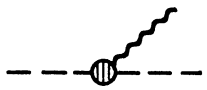

11

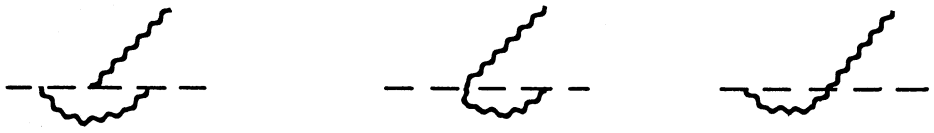

a b c

12

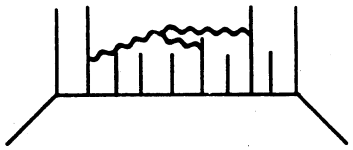

13

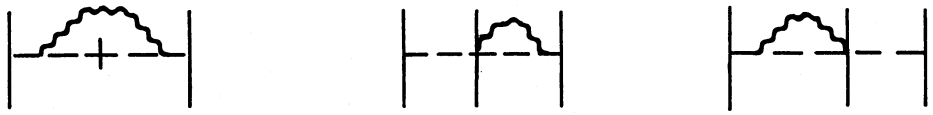

14

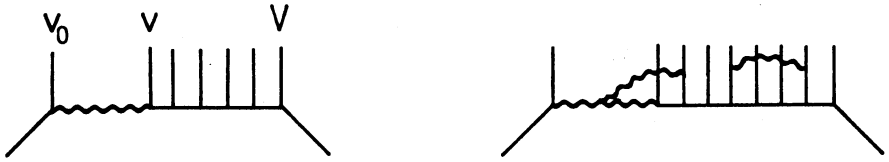

15

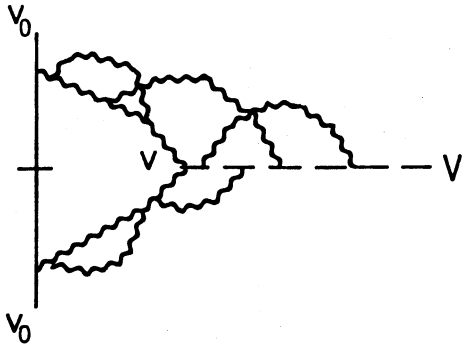

16

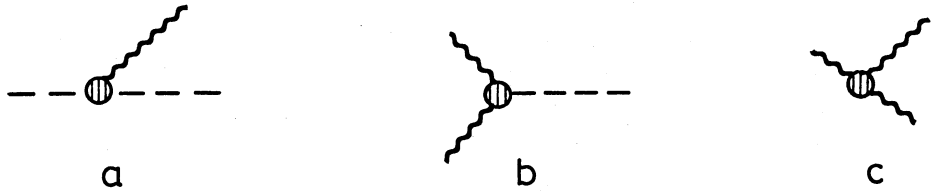

17

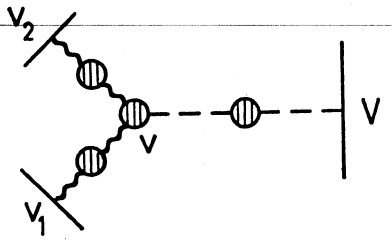

18

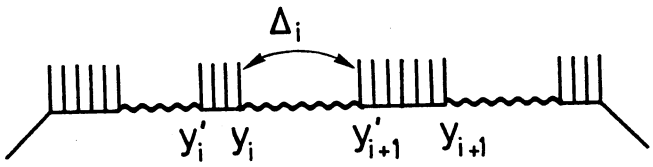

19

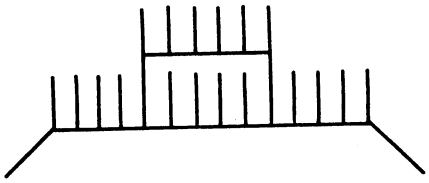

20

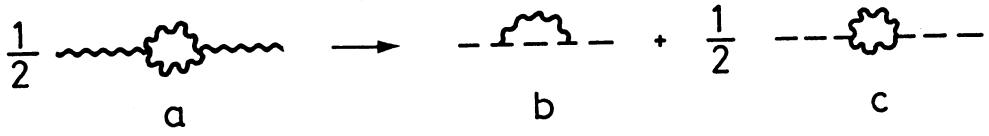

21